Nuclear Instruments and Methods in Physics Research A 816 (2016) 176–183

Contents lists available at ScienceDirect

Nuclear Instruments and Methods in Physics Research A

journal homepage: www.elsevier.com/locate/nima

Effect of Mg^{2+} ions co-doping on timing performance and radiation tolerance of Cerium doped $Gd_3Al_2Ga_3O_{12}$ crystals

M.T. Lucchini [a,*], V. Babin [c], P. Bohacek [c], S. Gundacker [a], K. Kamada [d,f], M. Nikl [c], A. Petrosyan [b], A. Yoshikawa [d,e,f], E. Auffray [a]

[a] CERN, 1211 Geneva 23, Switzerland
[b] Institute for Physical Research, Ashtarak, Armenia
[c] Institute of Physics AS CR, Prague, Czech Republic
[d] Tohoku University, New Industry Creation Hatchery Center, Sendai, Japan
[e] Tohoku University, Institute for Material Research, Sendai, Japan
[f] C&A Corporation, T-Biz, Sendai, Japan

ARTICLE INFO

Article history:
Received 21 December 2015
Received in revised form
29 January 2016
Accepted 1 February 2016
Available online 11 February 2016

Keywords:
Inorganic scintillators
Medical imaging
Calorimeters
Time-of-flight
Radiation tolerance

ABSTRACT

Inorganic scintillators with high density and high light yield are of major interest for applications in medical imaging and high energy physics detectors. In this work, the optical and scintillation properties of Mg co-doped Ce:$Gd_3Al_2Ga_3O_{12}$ crystals, grown using Czochralski technique, have been investigated and compared with Ce:$Gd_3Al_2Ga_3O_{12}$ ones prepared with identical technology. Improvements in the timing performance of the Mg co-doped samples with respect to Ce:$Gd_3Al_2Ga_3O_{12}$ ones have been measured, namely a substantial shortening of the rise time and scintillation decay components and lower afterglow were achieved. In particular, a significantly better coincidence time resolution of 233 ps FWHM, being a fundamental parameter for TOF-PET devices, has been observed in Mg co-doped crystals. The samples have also shown a good radiation tolerance under high doses of γ-rays, making them suitable candidates for applications in harsh radiation environments, such as detectors at future collider experiments.

1. Introduction

Inorganic scintillators combined with photodetectors are commonly used as efficient radiation detectors for applications in medical imaging and high energy physics [1–4]. In particular for time-of-flight positron emission tomography devices (TOF-PET) and light-based calorimeters at future colliders, a lot of efforts are being spent to improve the timing performance of such detectors. In the former case, the coincidence time resolution (CTR) represents a key parameter to improve noise suppression and to enhance signal to noise ratio in the reconstructed image [5–8]. In the latter, fast timing capabilities accompanied by a sufficient radiation tolerance of the scintillator would permit the detectors to operate in high rate conditions at future collider experiments [9,10].

In many inorganic scintillators such as Cerium-doped silicate and garnet single crystals the delayed radiative recombination at Ce emission centers due to electron traps can deteriorate scintillation performance leading to slow decay components and afterglow. In previous studies on Ce-doped orthosilicates (LSO, LYSO) [11,12], it was observed that Ca^{2+} co-doping can improve the scintillation characteristics due to the suppression of such undesired slow delayed recombination processes. Similar and very encouraging results were recently obtained with single crystal aluminum garnets (LuAG, YAG) by means of divalent ions co-doping such as Mg^{2+} and Ca^{2+} cations [13–15].

In recently discovered Ce:$Gd_3Al_2Ga_3O_{12}$ crystals (Ce: GAGG) [16,17] the defect-engineering of this kind to improve the scintillation mechanism has been applied as well. The detailed study of optical and scintillation characteristics of Ca co-doped GAGG:Ce single crystals and the Ca co-dopant effect on the stabilization of Ce^{4+} center in GAGG host has also been recently published [18]. Excellent scintillation properties of Ce:GAGG crystals and its relatively high density of 6.63 g/cm^3 make it a good candidate for radiation detectors.

Although previous publications have already started to study the properties of Mg- and Ca co-doped GAGG:Ce samples [17,18], the present study is focused on other crystal properties and their effects, which have not been investigated in the aforementioned

* Corresponding author.
E-mail address: Marco.Toliman.Lucchini@cern.ch (M.T. Lucchini).

http://dx.doi.org/10.1016/j.nima.2016.02.004

publications. In this paper we present the characterization of optical and scintillation properties of GAGG:Ce and GAGG:Ce:Mg samples grown by the Czochralski method. In particular, an improvement of the coincidence time resolution in GAGG:Ce:Mg crystals has been measured. Furthermore, an irradiation study using gamma-rays up to high doses ($\simeq 120$ kGy) has also been performed to investigate the radiation tolerance of such material.

2. Experimental methods and results

2.1. Crystal growth

Crystals of GGAG:Ce and GGAG:Ce:Mg were prepared by Czochralski method using an iridium crucible under N_2 atmosphere containing 2% O_2. The seed crystal of ⟨100⟩ orientation was purchased from C&A Corporation, Sendai, Japan. Mixtures of oxides of the purity 5N with compositions of $Gd_{2.985}Ce_{0.015}Ga_{2.7}Al_{2.3}O_{12}$ and $Gd_{2.982}Ce_{0.015}Mg_{0.003}Ga_{2.7}Al_{2.3}O_{12}$ were used as starting materials. A crystal growth velocity of 1.2 mm/hour was used and no excess of gallium oxide was added in the melt.

The set of samples used for the experiments consisted of a pair of GAGG:Ce and GAGG:Ce:Mg pixels ($2 \times 2 \times 10$ mm^3) and a pair of GAGG:Ce and GAGG:Ce:Mg cubes ($10 \times 10 \times 10$ mm^3). A BGO crystal in the form of $7 \times 7 \times 1$ mm^3 was also used for comparison in some of the measurements. The pixels were prepared from platelets which were cut perpendicularly to the crystal growth axis from the first third of the crystals whereas the cubes were obtained from the central part. All the faces of the samples were polished to optical quality.

Another couple of platelets, adjacent to those mentioned above, were analyzed using an electron micro-probe. The compositions of platelets from Mg-free and Mg co-doped crystals have been found to be $Gd_{3.09}Ce_{0.0027}Ga_{2.58}Al_{2.33}O_{12}$ and $Gd_{3.10}Ce_{0.0024}Mg_{0.0018}Ga_{2.54}Al_{2.36}O_{12}$ respectively. The distribution coefficients of Ce and Mg have been determined to be: $k_{Ce} = 0.14$ and $k_{Mg} = 0.45$.

The value of k_{Ce} we measured differs strongly from the one in [17], being 0.793. This is probably related to different growth methods (micro-pulling down in [17]) and different growth velocities, being 1.2 mm/h for our samples and 3.0 – 4.2 mm/h for the crystals in [17]. As the distribution coefficient approaches to 1 when the crystal growth velocity is increased [19], this could explain the larger value of k_{Ce} reported in [17].

2.2. Optical and scintillation properties

Absorption spectra, measured at Shimadzu 3101PC spectrometer across 2 mm thickness, are reported in Fig. 1 and show the $4f \rightarrow 5d^{1,2}$ transitions of Ce^{3+} center and the ^8S-^6P_x,^6I_x transitions of Gd^{3+}. In the Mg co-doped sample a clear fingerprint of Ce^{4+} charge transfer absorption is also observed, in agreement with previously published papers [12–14,18].

Transmission curves, measured at $10 \times 10 \times 10$ mm^3 cubes using a Perkin Elmer (Lambda 650 UV/VIS) spectrometer in the 200–800 nm range, are shown in Fig. 2. Both type of crystals have a good transmission of about 82% in the emission peak region (around 535 nm). The Mg co-doped samples show a stronger absorption in the UV region due to the presence of stable Ce^{4+} centers, see also Fig. 1 and related description.

Radio-luminescence spectra, in Fig. 3, were measured using a custom made 5000M Horiba Jobin Yvon spectrometer and an excitation X-ray source ISOVOLT 60 kV, Seifert Gmbh. A broad emission peak with the maximum around 530–535 nm was observed with no difference in the peak position between GAGG:Ce and GAGG:Ce:Mg samples. Absolute intensity of radio-luminescence is about 20% lower in the Mg co-doped samples, compared to Mg-free ones.

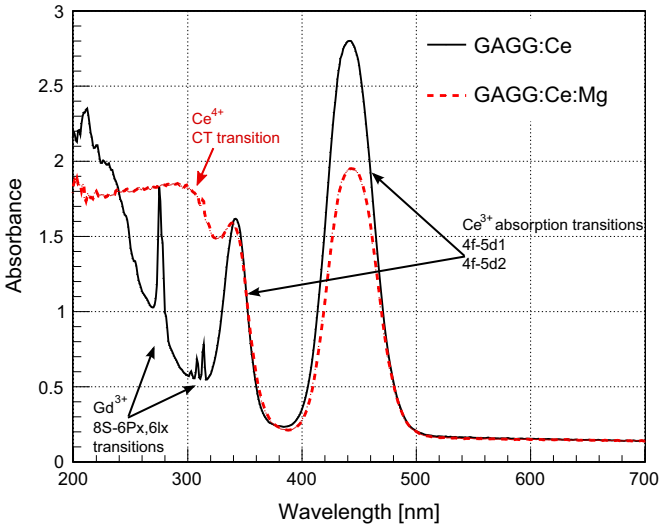

Fig. 1. Absorption spectra of GGAG:Ce and GGAG:Ce:Mg measured at $2 \times 2 \times 10$ mm^3 samples across 2 mm thickness.

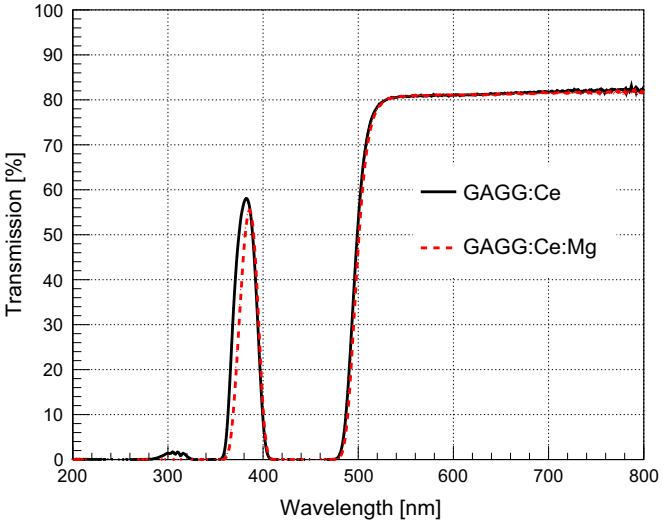

Fig. 2. Transmission curves for GAGG:Ce (black line) and GAGG:Ce:Mg (red dashed line) cubic samples. Lower transmission below 350 nm is observed for co-doped sample. (For interpretation of the references to color in this figure caption, the reader is referred to the web version of this paper.)

The light yield has been measured with a Photonics R2059 photomultiplier tube (PMT) under excitation by a ^{137}Cs source. Before measurement, the crystals were kept in the dark for one day to reduce the level of phosphorescence, see below Section 2.3. The samples were wrapped with Teflon tape and optically coupled with the PMT window using optical grease (refractive index $n = 1.41$). The quantum efficiency of the PMT weighed over the emission spectrum of GAGG:Ce was calculated to be $6.5 \pm 0.3\%$. The uncertainty on the light yield measurement, related to the error on the quantum efficiency calculation and to the calibration of the PMT, was estimated to be around 5%.

Light yield results are reported in Fig. 4 and summarized in Table 1. Using a 3 μs integration gate, a light yield of 35600 ± 1700 ph/MeV was measured for the GAGG:Ce cubic sample, whereas the Mg co-doped cubic sample shows a lower light yield of about 27800 ± 1400 ph/MeV. The energy resolution was found to be 7.1% and 7.6% respectively.

The light yield of the pixel samples was measured by collecting the light from the 2×2 mm^2 face. A light yield of 34700 ± 1700 ph/MeV and 26700 ± 1300 ph/MeV was obtained for the Mg-free

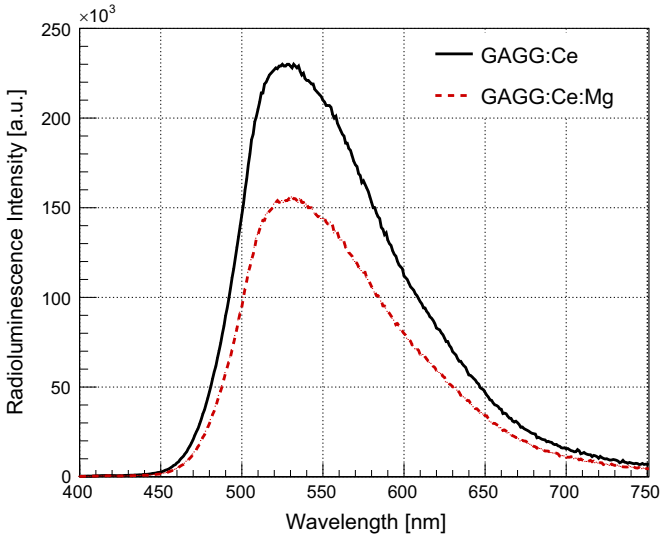

Fig. 3. Radio-luminescence spectra in absolute scale under excitation by X-ray tube (40 kV, 15 mA) for the GAGG:Ce and Mg co-doped GAGG:Ce crystals.

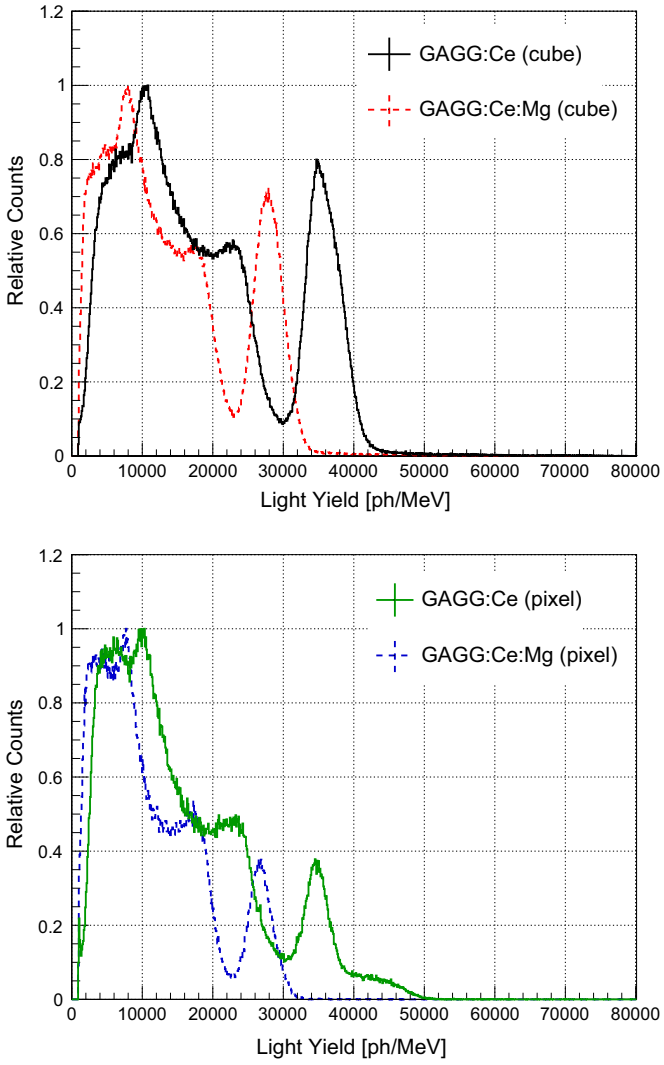

Fig. 4. Light yield spectra measured with optical grease couplant and Teflon wrapping for cubic samples (top) and pixel samples (bottom).

Table 1
Light yield and energy resolution measured using optical grease coupling and wrapping the samples with several layers of Teflon. A 3000 ns integration gate was used. Light yield for an LSO:Ce pixel of same dimensions was measured in the same configuration for comparison.

Shape	Crystal	LY (ph/MeV)	$\sigma_E/E(\%)$
Cube	GAGG:Ce	35600 ± 1800	7.1
Cube	GAGG:Ce:Mg	27800 ± 1400	7.6
Pixel	GAGG:Ce	34700 ± 1700	5.7
Pixel	GAGG:Ce:Mg	26700 ± 1300	5.9
Pixel	LSO:Ce	26500 ± 1300	5.5

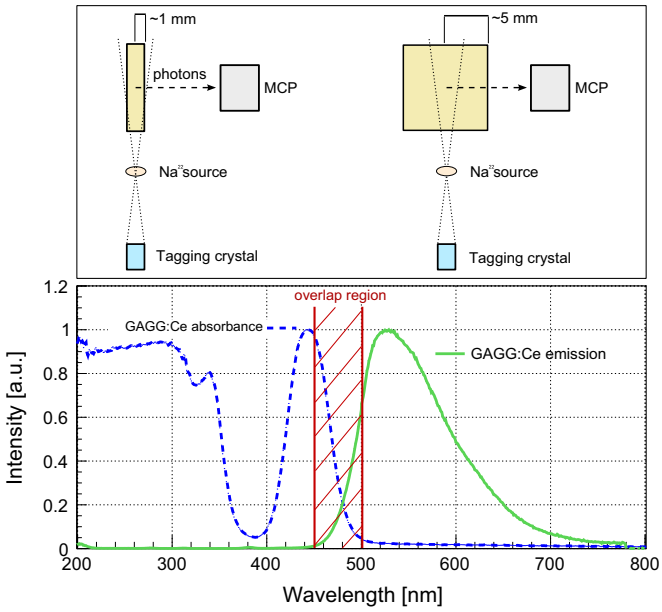

Fig. 5. Top: schematic view of the experimental setup used for measurement of decay time. Light has to travel a larger path inside the cubic samples because γ excitation occurs in the central region of the crystal volume. Bottom: comparison of absorption and emission spectra to show the overlap region around 480 nm, responsible for light self-absorption.

and Mg co-doped samples, respectively. The slightly lower light yield measured for the pixel geometry can be attributed to less efficient light collection. In high aspect ratio samples, photons undergo on average a larger number of reflections at the surface leading to a lower detection probability As shown in Table 1, the energy resolution of pixel samples is slightly better than that of cubic samples. This is likely to be related to the smaller volume of pixels in which the detection rate of photons produced by afterglow processes is lower. At the same time, in cubic samples the larger amount of photons originating from afterglow contributes to the degradation of the resolution as suggested by the non-Gaussian tail of light yield spectrum for the GAGG:Ce cube in Fig. 4. Light yield values and energy resolution measured on the Mg co-doped GAGG:Ce pixel and reported in Table 1 are comparable with the values achieved with a standard LSO:Ce pixel of same dimensions used as reference.

A comparison of the scintillation time profiles of the cubic and pixel samples is shown in Fig. 6. The decay time measurements were performed using the time correlated single photon counting setup [20] (see Fig. 5), in which we constrain events to the 511 keV photopeak on the start-detector. The start-detector is realized with a $2 \times 2 \times 5$ mm^3 LSO:Ce codoped 0.4% Ca scintillator from the producer Agile, and is coupled to a Hamamatsu S10931-050P

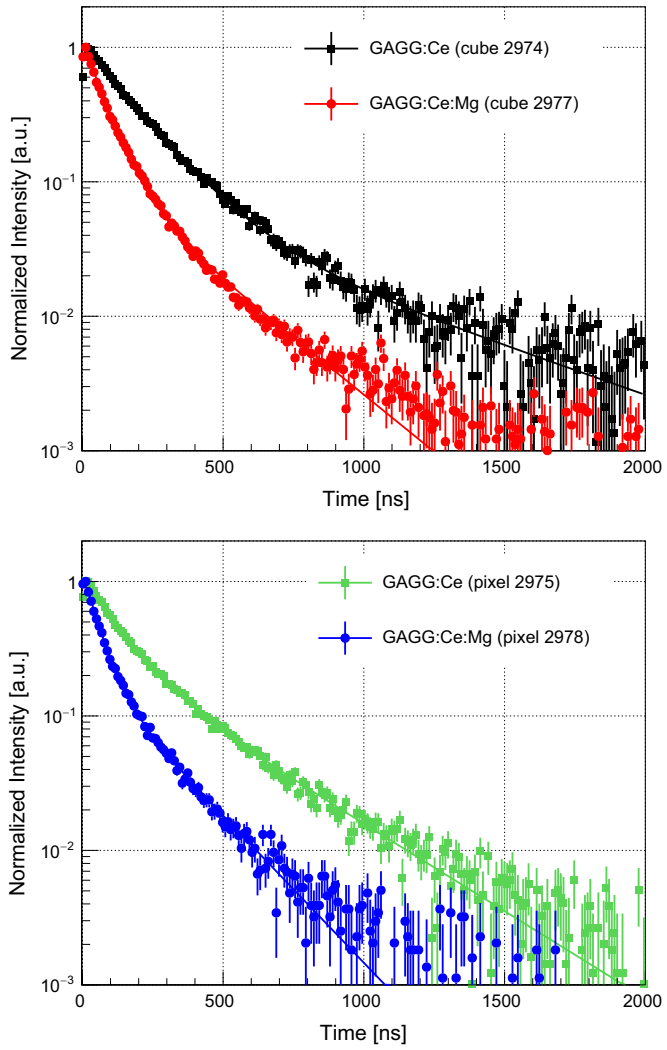

Fig. 6. Scintillation time profiles in 2000 ns gate, normalized to the maximum, measured for the cubic (top figure) and pixel samples (bottom figure) with and without Mg co-doping.

MPPC that is read out by the NINO chip, a low noise time-over-threshold comparator discriminator [21]. The stop-detector was realized with a Hamamatsu R3809U-50 series micro-channel plate photomultiplier tube (MCP-PMT) with a single photon time resolution of 25 ps FWHM.

A double-exponential fit was performed to estimate the decay time components according to the following parameterization:

$$A(t) = A_1 e^{-t/\tau_1} + A_2 e^{-t/\tau_2}$$

in which the relative intensity of the two components, in terms of total number of photons emitted, is given by

$$I_i = \frac{A_i \tau_i}{\sum A_i \tau_i}.$$

The results are reported in Table 2. The Mg co-doped crystals show a faster decay time with respect to GAGG:Ce crystals, confirming previous observations [17]. In particular the slow decay time component in Mg co-doped crystals appears to be strongly decreased.

Small differences between cubic samples and pixels can be observed. In particular the pixel geometry seems to have a slightly faster decay, which can be explained by the shorter average light path that photons have to travel inside pixels (with respect to cubic samples) before reaching the MCP-PMT. This is related to the particular setup which has been used for this measurement and reported in Fig. 5.

Table 2
Summary of decay time components (τ_i) with relative intensity (A_i) for cubic and pixel samples. The rise time measured on GAGG:Ce(Mg) pixels is also reported. Values for a LSO:Ce pixel of $2 \times 2 \times 10$ mm^2 are also shown for comparison and were measured in [22].

Shape	Crystal	$\tau_{d,1}$ (ns)	I_1 (%)	$\tau_{d,2}$ (ns)	I_2 (%)	τ_r (ps)
Cube	GAG:Ce	156	76	565	24	–
Cube	GAG:Ce:Mg	73	71	275	29	–
Pixel	GAG:Ce	101	65	319	35	1780
Pixel	GAG:Ce:Mg	51	53	196	47	54
Pixel	LSO:Ce	44	100	–	–	80

A shorter light path inside the crystal results in a lower probability of self-absorption (due to the overlap of the $4f \rightarrow 5d^1$ absorption and emission band of Ce^{3+}) [23]. Since, in the cubic samples, photons have to travel on average a 4 mm longer distance inside the crystal, the probability of self-absorption and re-emission is higher and leads to slower measured scintillation pulses. The influence of self-absorption on the luminescence decay profile is discussed in more detail in [24].

The rise time of the pixel samples was also measured using a single photon counting setup as described in [20,22]. The Mg co-doped crystal shows a rise time of $\tau_r = 49 \pm 20$ ps which is much faster than the value measured for standard GAGG:Ce sample, $\tau_r = 2263 \pm 40$ ps, as reported in Table 2 and shown in Fig. 7.

2.3. Afterglow and phosphorescence

For detectors which have to operate at high rate conditions, such as future collider experiments, afterglow and phosphorescence should be as low as possible to avoid the increase of equivalent noise with consequent degradation of signal-to-noise ratio [25].

In Fig. 8 the afterglow characteristics measured with the $2 \times 2 \times 10$ mm^3 samples are shown. Crystals were irradiated with X-rays and their luminescence was monitored immediately after the cut-off, for about 1400 ms. While the GAGG:Ce:Mg shows nearly three orders of magnitude decrease of signal in 10 ms after X-ray cut-off, GAGG:Ce shows a smaller decrease of about 40 times. The sample of BGO, which is known by its extremely low afterglow, shows a decrease of about four orders of magnitude. Very slow decrease of the afterglow signal in time suggest its existence also at much longer times which has been indeed observed as phosphorescence in GAGG:Ce sample in time scale of hours.

In order to estimate the magnitude of the phosphorescence decay and to compare the relative intensity between GAGG:Ce and GAGG:Ce:Mg crystals, the cubic samples have been irradiated with UV light (254 nm) for 2 hours. About 1 minute after UV-irradiation, the crystals were placed on top of Hamamatsu photomultiplier tube (PMT H6533) at a distance of 2 cm from the PMT window by mean of an opaque plastic holder which acted as a diaphragm of 4 mm diameter. The photons originating from delayed recombination processes and reaching the photodetectors have been measured by monitoring the PMT current during 24 hours after UV-irradiation. The results obtained are reported in Fig. 9 and show that the level of phosphorescence in Mg co-doped crystal is about an order of magnitude lower with respect to the reference GAGG:Ce sample.

A power-law fit was performed on the data to describe the intensity of phosphorescence, $I(t)$, at a given time t according to $I(t) = I(0)t^{-\alpha}$ as proposed in [26]. Such model can explain the

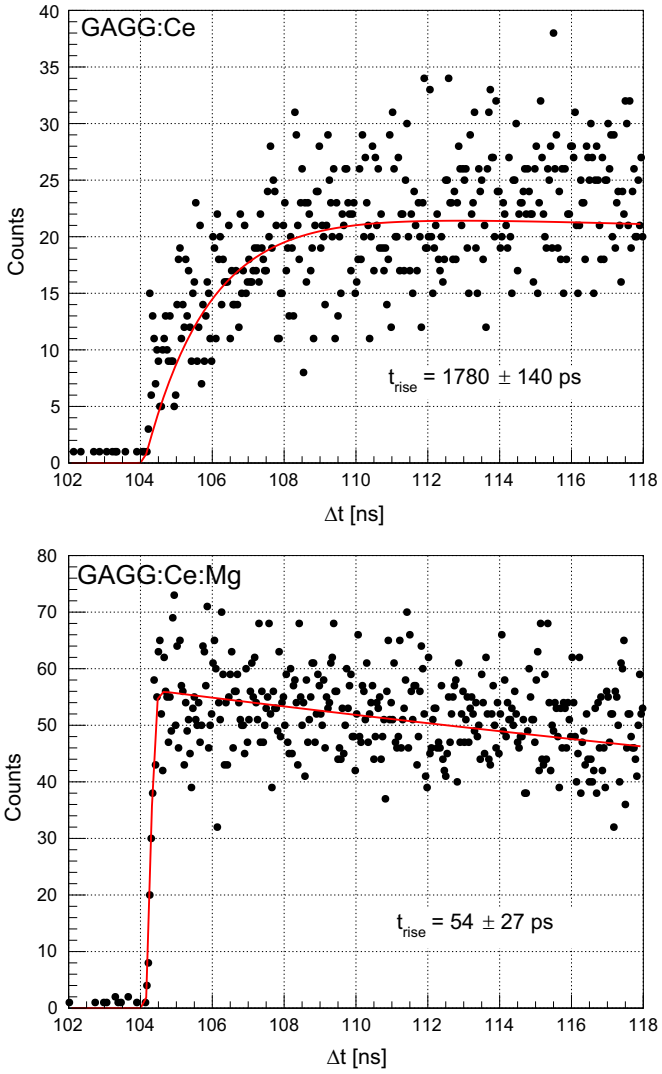

Fig. 7. Scintillation time profile in the first 15 ns, measured with the rise time setup. Fit function (red line) is superimposed to the data. (For interpretation of the references to color in this figure caption, the reader is referred to the web version of this paper.)

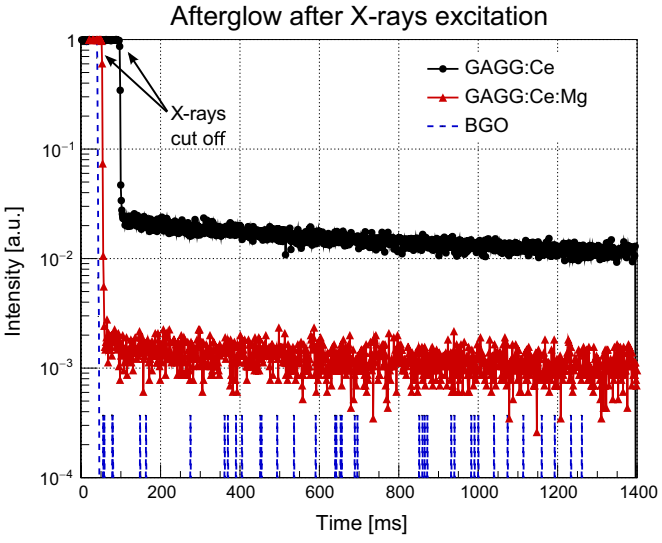

Fig. 8. Afterglow of the GAGG:Ce and GAGG:Ce:Mg samples in comparison with BGO crystal. Excitation by X-ray (1 min, 40 kV, 15 mA) was applied and its cut-off is marked in the graph.

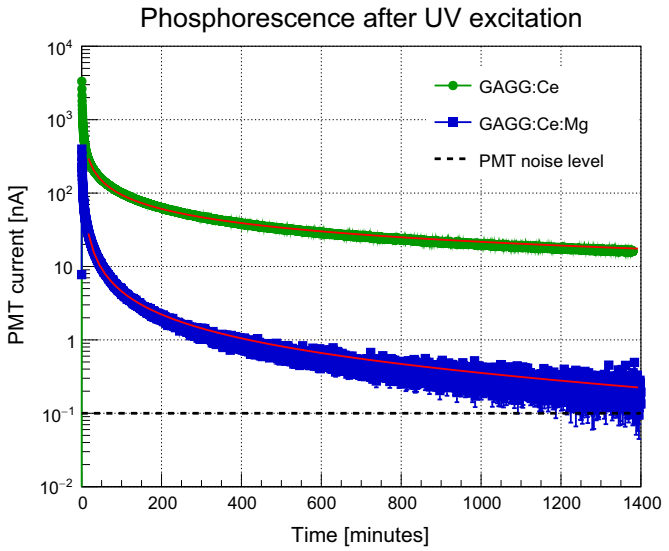

Fig. 9. PMT current induced by crystal phosphorescence after excitation with UV light. The GAGG:Ce crystal show a high level of phosphorescence whereas the Mg co-doped sample phosphorescence is more than one order of magnitude lower and close the PMT thermal noise level (black dashed line) after 24 hours.

Table 3
Fit parameters obtained for the phosphorescence curves shown in Fig. 9 are the GAGG:Ce and the Mg co-doped GAGG:Ce cubic samples.

Sample	$I(0)$	α
Mg-free	1806	0.64
Mg-doped	497	1.01

observed luminescence as the result of the tunneling of trapped electrons to recombination centres that are randomly distributed.

Results from the fit are reported in Table 3. In the Mg co-doped samples the intensity of phosphorescence is about 20 times lower than for Mg-free crystals and the corresponding α-coefficient is higher, indicating that relaxation of traps is faster. Small deviations, at the 5% level, from the power law curve are observed especially in the very first minutes of the phosphorescence decay, suggesting that more complex mechanisms are involved, e.g. a change in the spatial distribution of the distance between electron traps and recombination centres. Nevertheless, this measurement confirms the positive influence of Ce^{4+} centers in reducing the characteristic relaxation time of electron traps.

2.4. Coincidence time resolution

Coincidence time resolution (CTR) measurements were performed using the $2 \times 2 \times 10\ mm^3$ pixel samples. The setup consisted of two TSV (*through silicon via*) silicon photomultipliers (SiPM) of the Hamamatsu MPPC S12641-PA-50(X) type, operated at 3.8 V bias over-voltage. The former SiPM was coupled to a reference LSO crystal ($2 \times 2 \times 3\ mm^3$), the latter to the target GAGG:Ce pixel. Given CTR values are then always corrected for the reference time resolution, as if two similar GaGG:Ce crystals and SiPMs were used on both sides. The signal from the SiPM was collected through separate channels for time and energy information, ensuring best performance [27].

The CTR values obtained were 540 ± 40 ps FWHM and 233 ± 20 ps FWHM respectively for the GAGG:Ce and the GAGG:Ce:Mg crystal. Such result confirms the independent measurements of rise and decay time being faster for the Mg co-doped sample and thus leading to a better CTR. The CTR obtained with

the Mg co-doped sample is rather good if compared with the CTR of 156 ps measured on LYSO:Ce pixels of same dimensions as reported in [22].

2.5. Radiation tolerance

Radiation tolerance is a fundamental requirement for scintillators which have to operate in high radiation environments, such as detectors in future high energy colliders. In addition, γ-rays irradiation is a way to investigate the presence of impurities in the raw material and as-grown defects in the crystal structure which could be converted into color centers after irradiation.

A γ-rays irradiation study was thus performed on the cubic samples, having a geometry which is more suitable both for uniform irradiation and precise transmission measurements. The samples have been irradiated uniformly with γ-rays using a ^{60}Co source at the Institute for Physics Research (IPR) in Ashtarak. The crystals have been exposed to a total dose of 120 kGy at a dose rate of $\sim$0.6 kGy/h. Transmission curves were measured before, T_b, and after irradiation, T_a, in order to calculate the induced absorption coefficient as

$$\mu_{ind} = \frac{1}{L}\ln\left(\frac{T_b}{T_a}\right)$$

where L=1 cm is the thickness of the sample across which the light transmission is measured.

The irradiation results demonstrate that no creation of color centers occurs and that change in transmission above 530 nm is limited to the $\sim$1% level as reported in Fig. 10. In particular the Mg co-doped sample appears to have a lower induced absorption of $\mu_{ind} = 0.6 \pm 0.3\ \mathrm{m}^{-1}$ at the emission peak (535 nm) with respect to the standard GAGG:Ce crystal which has $\mu_{ind} = 1.5 \pm 0.3\ \mathrm{m}^{-1}$ as shown in Fig. 11. At low wavelengths (e.g. around 370 and 300 nm) the induced absorption coefficient is higher as previously observed on other Lutetium- and Yttrium-based garnets crystals [28,29].

3. Discussion

Distinct changes of scintillation properties in Mg co-doped GAGG:Ce crystals are observed with respect to GAGG:Ce ones. In particular, a decrease of light yield and a faster scintillation decay are measured for the former samples. This result is consistent with previous observations [17,18]. A faster decay can be explained by the stabilization of the Ce^{4+} centres, due to Mg co-doping, which provide an alternative channel for fast radiative de-excitation. The Ce^{4+} centres compete with any kind of electron traps in the material for the capture of an electron from the conduction band. This leads to a reduction of the intensity of slow radiative recombination processes. The decrease of light yield does not have an immediate explanation: for instance, in the Ca co-doped GGAG:Ce a comparatively bigger decrease of light yield was measured and the Ca-doping was found to induce a deep electron trap. In particular, a peak around 390 K, i.e. well above room temperature, was observed in the thermoluminescence glow spectrum [30]. If similar traps could be stabilized also in Mg co-doped GAGG:Ce, though in lesser extent, it could explain both the radioluminescence decrease in Fig. 3 and the lower light yield measured for these samples. This aspect needs, however, further study.

The measurements presented in this paper prove that a faster rise time of 54 ± 27 ps is obtained with Mg co-doped samples with respect to the relatively slow rise time of GAGG:Ce crystal 1780 ± 140 ps. This means that the overall timing performance of such co-doped samples is better as demonstrated by the

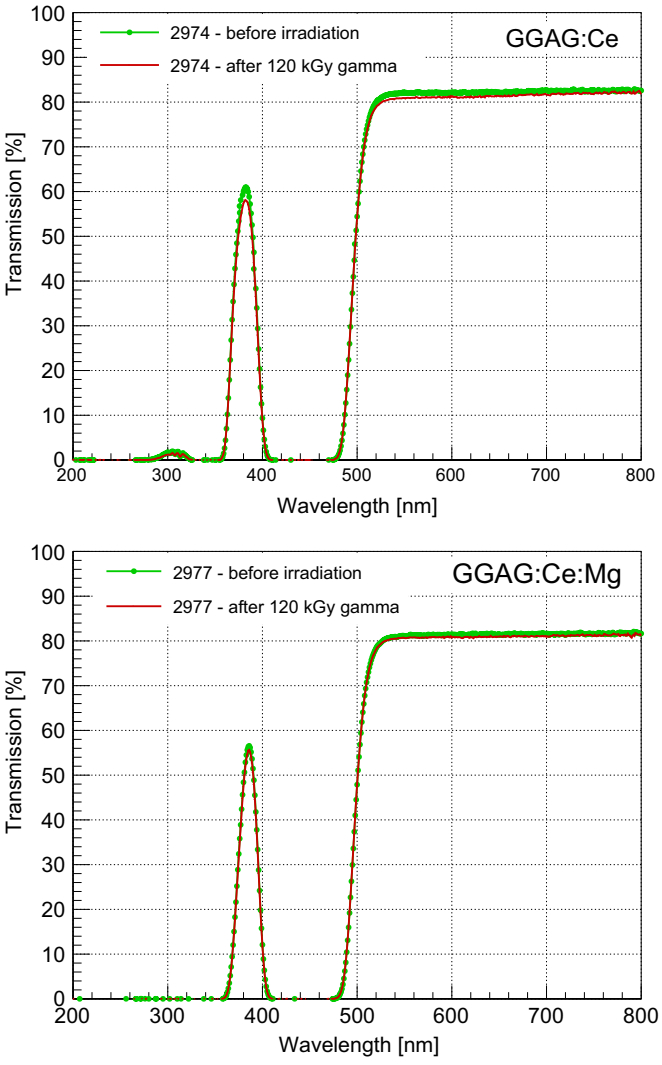

Fig. 10. Transmission curves of GAGG:Ce (top) and GAGG:Ce:Mg (bottom) samples before (green dots) and after irradiation with γ-rays up to 120 kGy (red line). (For interpretation of the references to color in this figure caption, the reader is referred to the web version of this paper.)

improvement observed in the CTR measurement. Of particular interest is the CTR of 233 ± 20 ps FWHM achieved with the Mg co-doped GAGG:Ce sample, being an encouraging result to motivates further investigation on the potential of this material for TOF-PET applications. Lower afterglow and phosphorescence signal in Mg co-doped GAGG:Ce are also of big advantage for practical applications.

A good radiation tolerance to γ-rays up to the cumulative dose of 120 kGy is also observed for both samples with no creation of specific color centers. This confirms the purity of the raw material and the quality of the crystal structure of the samples. The limited induced absorption in the range of the emission peak wavelength makes such crystals promising candidates for application in high energy and high radiation environments.

It was previously demonstrated for Gd_2SiO_5 (GSO), that despite gadolinium having a large thermal neutron cross-section, no degradation of transmission occurred up to the thermal neutron fluence of $10^{14}\ \mathrm{cm}^{-2}$ [31,32]. Due to its large cross-section for neutron capture, gadolinium provides an efficient way for thermal neutrons detection, which might be exploited to improve the

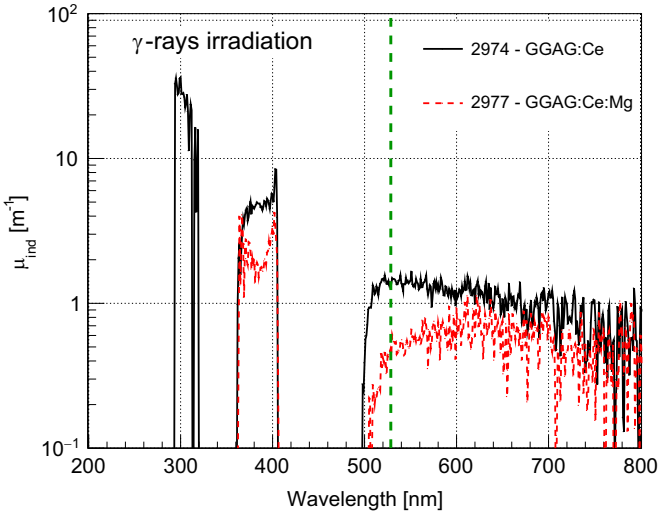

Fig. 11. Induced absorption coefficient after 120 kGy γ-rays irradiation for GAGG:Ce (black line) and GAGG:Ce:Mg (red dashed line). The μ_{ind} is shown only in the wavelength intervals where transmission is above 10% to allow for a reliable calculation of the induced absorption coefficient. Green dashed line shows the position of the emission peak at 535 nm. (For interpretation of the references to color in this figure caption, the reader is referred to the web version of this paper.)

energy resolution of hadronic calorimeters and neutron detectors in general, as previously investigated for GSO [33,34].

In high energy physics experiments, however, scintillation crystals are sometimes exposed to intense fluxes of high energy hadrons (protons, neutrons, mesons, etc.). Detectors exposed to such conditions may be subject to large integrated fluences of hadronic particles and thus suffer a response degradation. To investigate the radiation tolerance of GAGG:Ce crystals, to this type of radiation, further studies needs to be performed.

4. Conclusions

A set of Mg co-doped GAGG:Ce crystals grown by the Czochralski technique has been compared with Mg-free GAGG:Ce samples prepared by the same technology. An improvement of the timing performance in terms of faster rise and decay times of the scintillation pulse with consequent improvement of the coincidence time resolution down to 233 ± 20 ps has been observed. Taking into account the very high light yield and low afterglow, this suggests that Mg co-doped GAGG:Ce is a promising scintillator for timing devices in high energy physics and TOF-PET applications. These results combined with the characterization of other optical and scintillation properties of the samples confirm previous observations on the effects of Mg^{2+} ions co-doping in garnet crystals.

Very good radiation hardness of both type of samples under irradiation with gamma-rays up to 120 kGy has also been observed. The Mg co-doped crystal shows an induced absorption of $\mu_{ind} = 0.6 \pm 0.3\ m^{-1}$, being smaller than the reference crystal having $\mu_{ind} = 1.5 \pm 0.3\ m^{-1}$. Such radiation resistance makes GAGG:Ce crystal a promising candidate especially for high energy physics detectors which have to operate in harsh radiation environments.

Acknowledgments

This work was performed in the framework of the Crystal Clear Collaboration and received funding from the European Union's Horizon 2020 research and innovation program under the Marie Skodowska-Curie Grant agreement no. 644260 (Intelum) and from the ERC Advanced Grant no. 338953 (TICAL). Support has been received also from ASCIMAT project under Grant agreement no. 690599 and from COST Action TD1401 (FAST). We also acknowledge the support received by the Czech Science foundation P204/12/0805. This work is partially supported by Adaptable & Seamless Technology Transfer Program through Target-driven R & D (A-STEP), JST, Development of Systems and Technology for Advanced Measurement and Analysis, Japan Science and Technology Agency (JST) and New Energy and Industrial Technology Development Organization (NEDO).

References

[1] T. Budinger, et al., Nuclear Medicine and Biology 23 (1996) 659, http://dx.doi.org/10.1016/0969-8051(96)00063-7.
[2] CMS Collaboration, The CMS electromagnetic calorimeter project, Technical Design Report, CERN/LHCC 97-33 CMS TDR 4, 1997.
[3] W. Moses, et al., IEEE Transactions on Nuclear Science NS-46 (1999) 474, http://dx.doi.org/10.1109/23.775565.
[4] M. Nikl, et al., Measurement Science and Technology 17 (2006) R37, http://dx.doi.org/10.1088/0957-0233/17/4/R01.
[5] W.W. Moses, et al., IEEE Transactions on Nuclear Science NS-50 (2003) 1325, http://dx.doi.org/10.1109/TNS.2003.817319.
[6] M. Conti, et al., Physica Medica 25 (2009) 1, http://dx.doi.org/10.1016/j.ejmp.2008.10.001.
[7] S. Gundacker, et al., Nuclear Instruments and Methods in Physics Research Section A 737 (2014) 92, http://dx.doi.org/10.1016/j.nima.2013.11.025.
[8] M. Nemallapudi, et al., Physics in Medicine and Biology 60 (2015) 4635, http://dx.doi.org/10.1088/0031-9155/60/12/4635.
[9] CMS Collaboration, Technical proposal for the phase-ii upgrade of the compact muon solenoid, CERN-LHCC-2015-010, LHCC–P–008, 2015.
[10] A. Benaglia, et al., Detection of high energy muons with sub-20 ps timing resolution using L(Y)SO crystals and SiPM readout, Nuclear Instruments and Methods in Physics Research Section A (2016), in preparation.
[11] M.A. Spurrier, et al., IEEE Transactions on Nuclear Science NS-55 (2008) 1178, http://dx.doi.org/10.1109/TNS.2007.913486.
[12] S. Blahuta, et al., IEEE Transactions on Nuclear Science NS-60 (2013) 3134, http://dx.doi.org/10.1088/0031-9155/60/12/4635.
[13] M. Nikl, et al., Crystal Growth and Design 14 (2014) 4827, http://dx.doi.org/10.1021/cg501005s.
[14] A. Nagura, et al., Japanese Journal of Applied Physics 54 (2015) 04DH17, http://dx.doi.org/10.7567/JJAP.54.04DH17.
[15] A. Petrosyan, et al., Journal of Crystal Growth 430 (2015) 46, http://dx.doi.org/10.1016/j.jcrysgro.2015.08.019.
[16] K. Kamada, et al., Journal of Crystal Growth 352 (2012) 88, http://dx.doi.org/10.1016/j.optmat.2014.10.008.
[17] K. Kamada, et al., Optical Materials 41 (2015) 63, http://dx.doi.org/10.1016/j.optmat.2014.10.008.
[18] Y. Wu, et al., Physical Review Applied 2 (41) (2014) 044009, http://dx.doi.org/10.1103/PhysRevApplied.2.044009.
[19] B. Jindal, W. Tiller, The Journal of Chemical Physics 41 (1968) 4632, http://dx.doi.org/10.1063/1.1669923.
[20] L.M. Bollinger, et al., Review of Scientific Instruments 32 (1961) 1044, http://dx.doi.org/10.1063/1.1717610.
[21] S. Gundacker, et al., Sipm photodetectors for highest time resolution in pet, in: Proceedings of Science PoS (PhotoDet 2012) 016, LAL Orsay, 2012.
[22] S. Gundacker, et al., Measurement of intrinsic rise times for various l(y)so and luag scintillators with a general study of prompt photons to achieve 10 ps in tof-pet, Physics in Medicine and Biology (2015), in press.
[23] K. Pauwels, et al., IEEE Transactions on Nuclear Science NS-59 (2012) 2340, http://dx.doi.org/10.1109/TNS.2012.2183890.
[24] F. Auzel, et al., Optical Materials 24 (2003) 103, http://dx.doi.org/10.1016/S0925-3467(03)00112-5.
[25] E. Auffray, et al., IEEE Transactions on Nuclear Science NS-47 (2013) 1, http://dx.doi.org/10.1109/NSSMIC.2013.6829513.
[26] D.J. Huntley, Journal of Physics: Condensed Matter 18 (2006) 1359, http://dx.doi.org/10.1088/0953-8984/18/4/020.
[27] S. Gundacker, et al., Journal of Instrumentation 8 (2013) P07014, http://dx.doi.org/10.1088/1748-0221/8/07/P07014.

[28] M. Nikl, et al., Radiation damage processes in complex-oxide scintillators, in: Proceedings of SPIE, Damage to VUV, EUV, and X-ray Optics, vol. 6586, 2007, p. 65860E, http://dx.doi.org/10.1117/12.724737.
[29] M.T. Lucchini, et al., IEEE Transactions on Nuclear Science (2015), http://dx.doi.org/10.1109/TNS.2015.2493347, in press.
[30] M. Tyagi, et al., Journal of Physics D: Applied Physics 46 (2013) 475302, http://dx.doi.org/10.1088/0022-3727/46/47/475302.
[31] M. Kobayashi, et al., Nuclear Instruments and Methods in Physics Research Section A 330 (1993) 115, http://dx.doi.org/10.1016/0168-9002(93)91311-A.
[32] K. Kawade, et al., Journal of Instrumentation 6 (2011) T09004, http://dx.doi.org/10.1088/1748-0221/6/09/T09004.
[33] P.L. Reeder, Nuclear Instruments and Methods in Physics Research Section A 353 (1994) 134, http://dx.doi.org/10.1016/0168-9002(94)91619-5.
[34] D. Konish, et al., Nuclear Instruments and Methods in Physics Research Section A 420 (1999) 467, http://dx.doi.org/10.1016/S0168-9002(98)01173-5.